STREAMLINE CURVATURE CORRECTED ALGEBRAIC REYNOLDS STRESS TURBULENCE MODELLING

Stefan Wallin
Aeronautics Division, FFA
Swedish Defence Research Agency (FOI)
SE-172 90 Stockholm, Sweden
stefan.wallin@foi.se

Antti Hellsten
Helsinki University of Technology
FIN-02015 HUT, Finland
antti.hellsten@hut.fi

Markus Schatz & Thomas Rung
Hermann-Föttinger-Institute
Technical University Berlin
10623 Berlin, Germany
schatz@pi.tu-berlin.de

David Peshkin
QinetiQ
X80 building, Cody Technology Park
Farnborough GU14 0LX, England
dapeshkin@qinetiq.com

Arne V. Johansson
Department of Mechanics, KTH
SE-100 44 Stockholm, Sweden
johansson@mech.kth.se

ABSTRACT

A recently proposed curvature corrected explicit algebraic Reynolds stress model (CC-EARSM) based on a formal derivation of the weak-equilibrium assumption in a streamline oriented curvilinear co-ordinate system is further analysed and tested. The method is based on the rate of change of the strain-rate tensor following the mean flow and is fully three-dimensional, Galilean invariant and consistent in fully developed swirling flow. The predictive and numerical capabilities of the model are demonstrated using different standard non-commercial CFD solvers. The reduction of the Reynolds stresses in a zero-pressure gradient convex curved boundary layer and the inner wall in a U-duct flow due to the stabilising curvature is clearly shown. Moreover, the stabilising effect due to the swirl in a swirling combustor flow is significantly altering the swirl velocity component compared to the standard EARSM. In general, the curvature correction has been shown to significantly improve the results compared to the standard EARSM. In many cases, the results are close of these obtained using the full RSM. The curvature correction imposes some numerical problems and degenerates the convergence rate in some cases.

INTRODUCTION

Algebraic Reynolds stress models result from applying the weak equilibrium assumption on the full differential Reynolds stress models. In the weak equilibrium limit of turbulence, the Reynolds stress anisotropy tensor, $a_{ij} \equiv \overline{u_i u_j}/K - (2/3)\delta_{ij}$, is assumed to be constant following a streamline. Neglecting also the diffusion of the anisotropy tensor results in an implicit purely algebraic relation for a_{ij}, which may be formally solved resulting in an explicit relation (EARSM), see *e.g.* Pope (1975), Taulbee (1992), Gatski & Speziale (1993), Girimaji (1996) and Johansson & Wallin (1996).

The advection by the mean flow ($\mathrm{D}/\mathrm{D}t \equiv \partial/\partial t + U_k \partial/\partial x_k$) of a scalar field is zero if the scalar is homogeneous in the mean flow direction. However, the advection of a tensor field of higher rank than zero, *e.g.* vectors and second rank tensors, is not necessarily zero even if the flow is homogeneous in the mean flow direction.

This can be understood by transforming D/Dt to a general curvilinear co-ordinate system, $\boldsymbol{e}_i^s$, using the orthogonal transformation T_{ij} ($T_{ik}^t T_{kj} = \delta_{ij}$)

$$\frac{\mathrm{D}\, a_{ij}}{\mathrm{D}t} = T_{ip}^t \frac{\mathrm{D}\, a_{pq}^s}{\mathrm{D}t} T_{qj} - \left(a_{ik}\Omega_{kj}^{(\mathrm{r})} - \Omega_{ik}^{(\mathrm{r})} a_{kj} \right) \qquad (1)$$

where a_{ij} is $\boldsymbol{a}$ represented in the Cartesian co-ordinate system $\boldsymbol{e}_i = [\hat{\boldsymbol{x}}, \hat{\boldsymbol{y}}, \hat{\boldsymbol{z}}]$. The first term at the *r.h.s* is a differential term that represents the material derivative of the individual components of $\boldsymbol{a}$ represented in the system $\boldsymbol{e}_i^s$ (a_{ij}^s) and the second term is a purely algebraic term resulting from the curvilinear co-ordinate transformation where $\Omega_{ij}^{(\mathrm{r})}$ is directly related to the transformation through

$$\Omega_{ij}^{(\mathrm{r})} = \frac{\mathrm{D}\, T_{ik}^t}{\mathrm{D}t} T_{kj} = -T_{ik}^t \frac{\mathrm{D}\, T_{kj}}{\mathrm{D}t} \qquad (2)$$

Girimaji (1997) and Sjögren (1997) realized that the additional algebraic term may be written in terms of an antisymmetric tensor $\Omega_{ij}^{(\mathrm{r})}$, which represents the rotation of the $\boldsymbol{e}_i^s$ system following the streamline. This term can easily be accounted for in the EARSM solution by modifying the absolute vorticity tensor Ω_{ij} resulting in a "curvature corrected" model, CC-EARSM.

If the flow is homogeneous in the mean flow direction, *e.g.* in fully developed swirling flows, the differential term, the first term at the *r.h.s* of (1) represented in an appropriate co-ordinate system, will vanish. The non-zero $\mathrm{D}\boldsymbol{a}/\mathrm{D}t$ will, thus, be exactly represented by the second algebraic term, which represents the variation of the components of $\boldsymbol{a}$ due to the rotation of the principal directions following the mean flow.

In general flows which contain regions of strong swirl or streamline curvature, we cannot in advance choose the optimal co-ordinate system, so we need to find a method of

deriving the measure of the co-ordinate system rotation rate $\Omega_{ij}^{(r)}$ from the flow field. Only a few Galilean invariant methods have been proposed. Girimaji (1997) proposed to use the rotation rate of the acceleration vector and Gatski & Jongen (2000) used the rotation rate of the principal direction of the strain-rate tensor. However, these methods were only derived for 2D flows.

Hellsten (2002) has found that the acceleration based method leads to problems in some situations of mild curvature where the direction of the acceleration vector may vary rapidly. This was demonstrated in a U-bend flow, which showed an almost singular behaviour. For the same case, the strain-rate based method behaves much better.

Recently, Wallin & Johansson (2002) proposed a fully three-dimensional method based on the strain-rate tensor, which will be examined and tested in this study. In two-dimensional mean flows, the method by Wallin & Johansson reduces to the Gatski & Jongen (2000) correction. In fully developed swirling flows, which is fully three dimensional, the proposed method has been shown to be identical to the exact transformation.

Turbulent flows over curved surfaces, near stagnation and separation points, in vortices and turbulent flows in rotating frames of reference are all affected by streamline curvature effects. Strong curvature and/or rotational effects form a major cornerstone problem also at the Reynolds stress transport modelling level. Some of the effects of streamline curvature or local rotation is captured already in standard EARSMs. *E.g.* the Coriolis term that appears when transforming the Reynolds stress transport model equation to a rotating frame is composed by two equal parts that originate from the transformation of the production and the advection respectively. The production part is naturally captured also in standard EARSMs while the advection part is not.

In cases with moderately curved streamlines the neglection of the advection part has a rather minor effect, see *e.g.* Rumsey, Gatski & Morrison (1999) for flow over an airfoil, but in other cases the inclusion of the curvature correction is significant. That is the case in *e.g.* vortices (Wallin & Girimaji 2000), in rotating flows like rotating homogeneous shear and rotating channel (Wallin & Johansson 2002) and in curved channels as well as in swirling flows, as will be seen in this paper.

CURVATURE-CORRECTED MODEL

The curvature corrected EARSM (CC-EARSM) proposed by Wallin & Johansson (2002) will be repeated herein for clarity. It is based on a formal approximation of a Reynolds stress transport model including an approximation of the advection of the anisotropy.

General quasi-linear Reynolds stress transport models may be written in terms of a transport equation for the anisotropy tensor

$$\begin{aligned}\tau\left(\tfrac{\mathrm{D}\,a_{ij}}{\mathrm{D}t}-\mathcal{D}_{ij}^{(a)}\right) = A_0\Big[&\left(A_3+A_4\tfrac{\mathcal{P}}{\varepsilon}\right)a_{ij}\\ &+A_1 S_{ij}-\left(a_{ik}\Omega_{kj}-\Omega_{ik}a_{kj}\right)\\ &+A_2\left(a_{ik}S_{kj}+S_{ik}a_{kj}-\tfrac{2}{3}a_{kl}S_{lk}\delta_{ij}\right)\Big]\end{aligned} \tag{3}$$

see Wallin & Johansson (2000). $\mathcal{D}_{ij}^{(a)}$ is the diffusion of a_{ij} and $\tau = K/\varepsilon$ is the turbulent time-scale. The strain and rotation rate tensors, S_{ij} and Ω_{ij}, are normalized by τ. This relation results from the general quasi-linear model for the pressure-strain rate and dissipation rate anisotropy, e_{ij},

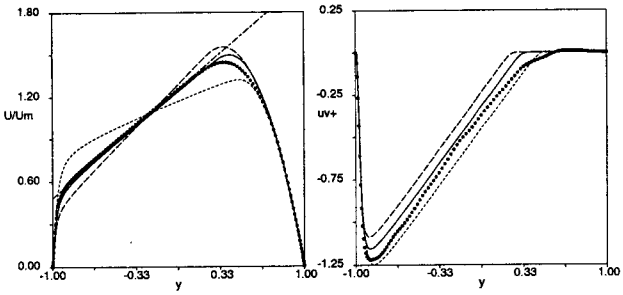

Figure 1: Computed rotating channel flow for $Ro = 0.77$ compared to DNS of Alvelius & Johansson (2000). Curvature corrected original (– – –) and recalibrated (——) WJ EARSM compared to the non-corrected EARSM (·····). $U' = 2\omega_z^{(r)}$ (–·–·–) is also shown. (figure taken from Wallin & Johansson, 2002)

lumped together

$$\begin{aligned}\tfrac{\Pi_{ij}}{\varepsilon}-e_{ij} = &-\tfrac{1}{2}\left(C_1^0+C_1^1\tfrac{\mathcal{P}}{\varepsilon}\right)a_{ij}+C_2 S_{ij}\\ &+\tfrac{C_3}{2}\left(a_{ik}S_{kj}+S_{ik}a_{kj}-\tfrac{2}{3}a_{kl}S_{lk}\delta_{ij}\right)\\ &-\tfrac{C_4}{2}\left(a_{ik}\Omega_{kj}-\Omega_{ik}a_{kj}\right).\end{aligned} \tag{4}$$

The A coefficients are related to the C coefficients through

$$\begin{aligned}A_0 = \tfrac{C_4}{2}-1,\quad A_1 = \tfrac{3C_2-4}{3A_0},\quad A_2 = \tfrac{C_3-2}{2A_0},\\ A_3 = \tfrac{2-C_1^0}{2A_0},\quad A_4 = \tfrac{-C_1^1-2}{2A_0}.\end{aligned} \tag{5}$$

Introducing the curvature correction for the original choice of the A_0 coefficient in the Wallin & Johansson (2000) model leads to a model that predicts rotational effects poorly as shown by Wallin & Johansson (2002) and also observed by Wallin & Girimaji (2000) for the vortex flow. Wallin & Girimaji found that the WJ model behaviour was improved by increasing A_0 to a value closer to that of the linearized SSG.

A more thorough analysis of the effect of the A_0 coefficient was done by Wallin & Johansson (2002), where the long time asymptotic behaviour in rotating homogeneous shear flow was considered. Depending on the rotation number the turbulent kinetic energy grows exponentially with constant $\mathcal{P}/\varepsilon$ or follows a power-law solution where $\varepsilon/(U_y K) \to 0$ (Speziale & Mac Giolla Mhuiris 1989). The bifurcation points between the two solution branches correspond to the points where $C_\mu^{(\mathrm{eff})}$ becomes zero or where the flow is close to neutral stability. Neutral stability occurs near rotation number $Ro = 0.5$ and is also likely associated with the linear velocity profile in the core of a rotating channel (local $Ro{\approx}0.5$) according to Pettersson-Reif *et al.* (1999). Thus, the model coefficients are calibrated such that the required bifurcation point $Ro = 0.5$ is obtained. The A coefficients proposed by Wallin & Johansson (2002) are $A_0 = -0.72$, $A_1 = 1.20$, $A_2 = 0$, $A_3 = 1.80$ and $A_4 = 2.25$.

The recalibrated model is tested in rotating channel flow in figure 1. Both the curvature correction and the recalibration are of significant importance in predicting the slope of the mean flow velocity profile in the centre of the channel. Also the relaminarization at the stabilized side is captured.

Strain rate based curvature correction

The advection of the strain rate tensor $\boldsymbol{S}$ may, similarly to the advection of the anisotropy tensor (1), be expressed as a differential plus an algebraic term arising from the trans-

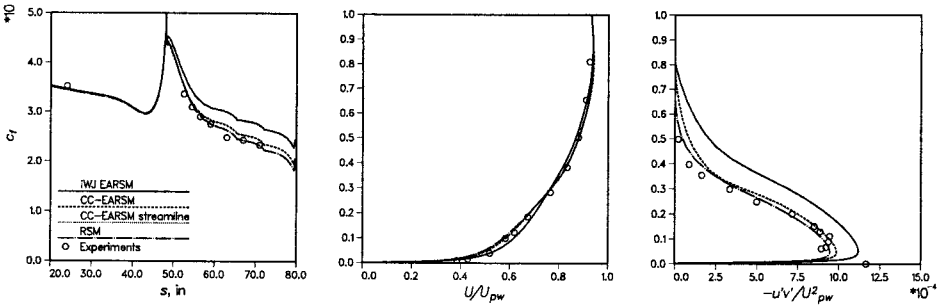

Figure 2: The skin-friction coefficient along the convex wall, the velocity profile and turbulent shear stress at $s = 71$ in. Experiment by So & Mellor (1973). The stresses are transformed into the local wall-tangential and -normal coordinate system, and U_{pw} is the theoretical potential velocity on the wall.

formation to the curvilinear co-ordinate system, $\boldsymbol{e}_i^s$

$$\frac{\mathrm{D}\,S_{ij}}{\mathrm{D}t} = T^t_{ip}\frac{\mathrm{D}\,S^s_{pq}}{\mathrm{D}t}T_{qj} - \left(S_{ik}\Omega^{(\mathrm{r})}_{kj} - \Omega^{(\mathrm{r})}_{ik}S_{kj}\right) \qquad (6)$$

The assumption made by Wallin & Johansson (2002) was that, since the anisotropy and the strain rate tensors are related, the co-ordinate system for which the differential part of the advection of $\boldsymbol{S}$ is minimized is used also for transforming the advection of the anisotropy. This may be obtained by finding the solution for the $\boldsymbol{\Omega}^{(\mathrm{r})}$ tensor from (6) where the first term on the *r.h.s.* is set to zero. However, that equation system is overdetermined since there are five (two in 2D) independent equations for $\mathrm{D}\boldsymbol{S}/\mathrm{D}t$ and three (one in 2D) independent components of $\boldsymbol{\Omega}^{(\mathrm{r})}$.

By using that $\Omega^{(\mathrm{r})}_{ij} \equiv -\epsilon_{ijk}\omega^{(\mathrm{r})}_k$ the equation for the advection of the transformed S_{ij} in (6)) becomes

$$e_{ij} \equiv T^t_{ip}\frac{\mathrm{D}\,S^s_{pq}}{\mathrm{D}t}T_{qj} = \frac{\mathrm{D}\,S_{ij}}{\mathrm{D}t} - \left(S_{il}\epsilon_{ljk} + S_{jl}\epsilon_{lik}\right)\omega^{(\mathrm{r})}_k \qquad (7)$$

e_{ij} may be minimized in a least square sense by minimizing the norm $e_{ij}e_{ij}$, which, for this case, is equivalent with $S_{pl}e_{lq}\epsilon_{pqi} = 0$. That results in the following expression for the rotation vector $\omega^{(\mathrm{r})}_i$

$$\omega^{(\mathrm{r})}_i = A_{ij}S_{pl}\frac{\mathrm{D}\,S_{lq}}{\mathrm{D}t}\epsilon_{pqj} \qquad (8)$$

where

$$A_{ij} = \frac{II_S^2\delta_{ij} + 12III_S S_{ij} + 6II_S S_{ik}S_{kj}}{2II_S^3 - 12III_S^2}. \qquad (9)$$

The denominator in (9) may become zero when two of the eigenvalues are equal or all eigenvalues are zero. The singularities at these points may be avoided by adding a small number to the denominator.

In two-dimensional incompressible mean flows, $\omega^{(\mathrm{S})}_i$ reduces to

$$\omega^{(\mathrm{r})}_3 = \frac{S_{11}\dot{S}_{12} - S_{12}\dot{S}_{11}}{2S^2_{11} + 2S^2_{12}} \qquad (10)$$

which is identical to the Spalart & Shur (1997) and the Gatski & Jongen (2000) corrections.

Implementation aspects

The strain-rate based curvature correction methods involve numerical approximation of $\mathrm{D}\boldsymbol{S}/\mathrm{D}t$. In steady-state problems (time-dependent problems not considered here) the derivative of the $\boldsymbol{S}$ tensor may be expressed in conservative form as

$$U_k\frac{\partial S_{ij}}{\partial x_k} = \frac{1}{\rho}\frac{\partial}{\partial x_k}\left(\rho S_{ij}U_k\right) = \frac{1}{\rho V}\oint_S \rho S_{ij}U_k\hat{n}_k\mathrm{d}S \qquad (11)$$

where S is the control volume surface and $\hat{n}_i$ is the unit normal vector of the control surface. In this formulation, the different components of $\mathrm{D}\boldsymbol{S}/\mathrm{D}t$ may be computed directly without the need of evaluating all components of the gradient of $\boldsymbol{S}$.

The velocity gradient components are computed onto each face of a control-volume or cell using local staggered cells. The derivatives of the strain-rate components are then computed in the cell centrepoints. This way the numerical error can, in principle, be kept small. However, spatially oscillating distribution of $\mathrm{D}\boldsymbol{S}/\mathrm{D}t$ may be obtained, especially when high-resolution grids are employed. Presently, this problem is handled by applying a spatial filter for the computed rotation vector $\boldsymbol{\omega}^{(\mathrm{r})}$. A top-hat filter of the width of three computational cells in each direction is employed. This turned out to be a sufficient remedy in the two-dimensional flows considered in this study. In the three-dimensional swirling flow, some spatial oscillation still occurs in the recirculation zone, but this neither prevents the iteration from converging nor spoils the results. It is felt, however, that the numerical computation of $\mathrm{D}\boldsymbol{S}/\mathrm{D}t$ still needs some further attention.

TEST CASES

Two-Dimensional Boundary Layer on a Convex Wall

A convex curved boundary layer experimentally studied by So & Mellor (1973) will be used for basic validation of the curvature corrected EARS-modelling. The concave outer wall is contoured to obtain a nearly constant pressure distribution on the inner wall. The CC-EARSM will be tested using two different ways to obtain $\omega^{(\mathrm{r})}_3$: the Wallin & Johansson (2002) strain-rate based method (8), which reduces to Eq. (10) in two-dimensional mean flows, and the streamline method in which $\omega^{(\mathrm{r})}_3$ is simply the rotation rate of the velocity vector following a streamline. The latter method is not generalizable due to its lack of Galilean invariance, but can be used as a reference here because the coordinate system can be attached to the apparatus. The results will be compared with the experimental data, with the results obtained with the standard EARSM derived in the inertial coordinate system (iWJ), and with full differential Reynolds stress model (RSM) predictions using the corresponding pressure-strain model, see Hellsten *et al.* (2002) and Salo (2003).

The skin-friction coefficient along the convex wall is shown in figure 2. Clearly, both CC-EARSMs as well as the RSM agree well with the measurements while the standard EARSM slightly overestimates the wall shear-stress as expected. The velocity and turbulent shear-stress distributions are also shown in the figure. The differences in the

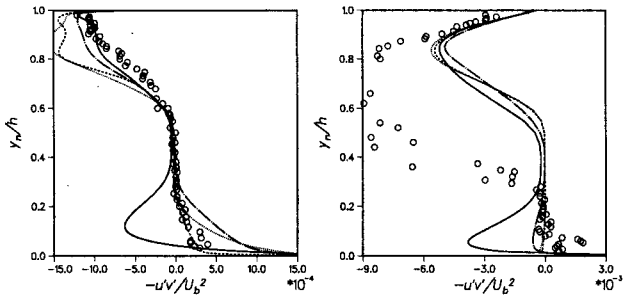

Figure 3: Turbulent shear stresses for the U-duct flow, in the beginning of the curved part, $\theta = 0$ deg (left), and in the middle of it, $\theta = 90$ deg (right). The stresses are transformed into the local wall-tangential and -normal coordinate system. Legends as in figure 2.

velocity profiles are quite small, while the shear-stress distributions reveal the differences more clearly. The turbulent shear stress $-\overline{uv}$ is damped by the curvature effect. This damping effect is most pronounced in the outer part of the boundary layer. The RSM and the CC-EARSMs capture this effect quite accurately in this case, while the standard EARSM captures it only partially. This is clear, because the streamline curvature enters in the RSM in two terms, the production and the advection. The standard EARSM only involves the former effect while the idea behind the curvature correction technique is to approximate the latter one. The choice of the method to approximate $\omega_3^{(r)}$ makes no difference in this case. The curvature correction seem to not remarkably affect the stability and the convergence rate of the computations in this particular case.

Plane U-Duct Flow

The plane U-duct flow experimentally studied by Monson & Seegmiller (1992) is a flow with much stronger curvature effect, since the radius of curvature is of the same order as the length scale of turbulence. In addition to the streamline curvature, there are strong pressure gradients, flow separation, and some three-dimensional phenomena.

Computations are performed using the same models as for the So & Mellor flow. The differences in the velocity profiles are almost negligibly small, especially, in the first two stations. This is because the pressure-gradient strongly dominates over the Reynolds-stress gradient in the mean-momentum equations.

The Reynolds shear-stress profiles are shown in figure 3 at two locations. There are large differences between the predicted shear stresses already in the beginning of the curved part. The strain-rate based correction allows best agreement with the measurements near the convex wall. The streamline correction and the RSM also give shear-stress profiles quite close to the measured data. The standard EARSM predicts a shear-stress profile that largely follows the strain rate and is therefore of opposite sign with the experimentally observed values, except in the immediate vicinity of the wall. The effect of the curvature correction here is primarily to reduce the coefficient of the first-order term $\beta_1 S_{ij}$ in the EARSM. Owing to this reduction, the second-order term

$$\beta_4 \left(S_{1k}\Omega^*_{k2} - \Omega^*_{1k}S_{k2} \right) = \beta_4 \Omega^*_{12} \left(S_{11} - S_{22} \right) \qquad (12)$$

becomes dominating. As a result of this, the right sign and magnitude is predicted for the shear stress in this area. Near

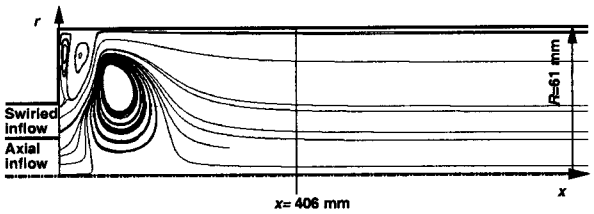

Figure 4: An illustration of the swirling combustor by Roback and Johnson (1983) with a typical streamline pattern (projected onto the plane). Vertical line indicates the location where the velocity profiles are studied. Note the horizontal shrinking of the image.

the outer wall, the CC-EARSM variants seem to overestimate the shear stress to some extent in this station.

In the middle of the curved duct ($\theta = 90$ deg), the shear stress is almost zero on the inner side, except in the near-wall region. This is also in a quite good agreement with the experiments. The RSM predicts a small amount of positive shear stress while the CC-EARSM variants give practically zero shear stress in this region. The computations also reveal that, according to the RSM and the CC-EARSMs, the reversal of the normal-stress anisotropies takes place in this region, that is, $\overline{vv} > \overline{uu}$. This phenomenon is known to occur in shear flows subjected to rapid destabilizing spanwise rotation, see, for example, Bech & Anderson (1997). On the outer side of the duct, all models agree with each other reasonably well in this station. However, the predicted shear stresses are by far too low in comparison with the experiments. This difference is likely due to streamwise Taylor-Görtler vortices typically found in concave-curved boundary layers, see Monson *et al.* (1990). Such vortices should be distinguished from the turbulent motion, because they are quite deterministic in structure. The present two-dimensional computations obviously do not capture such vortices, and the turbulence models are not designed to model such non-turbulent instabilities. The effect of these vortices is, however, included in the measured stresses.

In this case, the use of the curvature correction seems to reduce the numerical stability and the convergence rate to some extent, but not intolerably much.

Three-Dimensional Swirling Flow in a Model Combustor

Swirling flows involve additional strain components which may significantly influence the turbulence. The eddy-viscosity models are known to be unable to correctly capture these effects. The sensitivity of the algebraic Reynolds-stress models to the swirl effects is dependent on the coordinate system in which the weak-equilibrium assumption is made just like the sensitivity to planar curvature. Swirling flow is merely a more complex example of a curved flow. Here we will study the model combustor flow experimentally studied by Roback & Johnson (1983). The geometry and the flow are axisymmetric and the swirl velocity is induced by the inflow boundary conditions, see figure 4. The computational domain begins from the inlet plane and extends several tens of chamber diameters downstream of the interesting area. The details of the computational parameters are given by Hellsten *et al.* (2002).

The CC-EARSM will be tested using two different ways to obtain $\omega_i^{(r)}$: equation (8), and a simplified streamline method that accounts for the swirl velocity-component only.

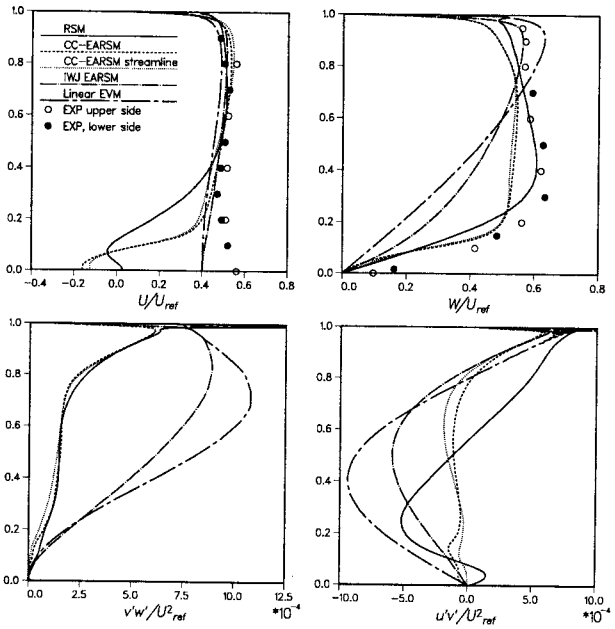

Figure 5: Velocity and shear-stress distributions in the model combustor in the station $x = 406$ mm.

Owing to the axisymmetry, this is simply

$$\omega_i^{(r)} = \delta_{i1} \frac{W}{r} \tag{13}$$

where r is the local radius from the axis of revolution. In the downstream part of the chamber, the radial velocity component and the axial derivatives are small, and the correction should then approach that of equation (13). Close to the inflow plane, (13) is expected to be in error, and the θ-component of the rotation rate becomes non-zero due to curvature in the $x - r$ plane. See Hellsten *et al.* (2002) for more results. The CC-EARSM results will be compared with the experimental data, with results computed using an RSM, with standard iWJ EARSM results, and with linear eddy-viscosity results. The RSM used in this case is not exactly the parent model of the EARSM, but it is close to it. This particular RSM is of general linear type and the model coefficients are reported by Rung *et al.* (1999) in context of another algebraic model derived from it.

The axial and circumferential mean-velocity components as well as the shear-stress components $\overline{uv}$ and $\overline{vw}$ are shown in figure 5 in the station $x = 406$ mm, see figure 4. An excessive axial velocity defect on the axis of revolution predicted by the CC-EARSMs and by the RSM is a salient feature. The linear eddy-viscosity model (EVM) predicts a linear rise of the azimuthal velocity similar to a solid-body motion. The standard iWJ EARSM can handle the curvature effect on production processes which lead to slightly better but still qualitatively wrong azimuthal velocity profile. A suitable prediction of all relevant effects is maintained by the full differential Reynolds stress model without the assumption of local equilibrium. This model can tackle streamline curvature and gives a good representation of the velocity profiles. The CC-EARSM using (8) as well as the a priori curvature correction according to (13) leads to results of almost the same quality as that of the RSM. The most important shear stress $\overline{vw}$ in the regions of low strain-rate downstream the recirculation is in a very good agreement with that obtained by the RSM.

The outflow conditions that do not properly model the experimental setup are probably the origin of the axial velocity dip on the axis. The high swirl rate induces low pressure near the axis and this makes the flowfield very sensitive to the outflow conditions. The experimental setup featured an endplate at $x \approx 1000$ mm and an exhaust duct mounted in 90 deg. angle relative to the chamber axis. This was not known at the time of the computations. Attempts to better simulate the outflow will be left for the future work.

The convergence rates of all computations in this case were slow. This is partially owing to the stiffness introduced by the very long computational domain. The strain-rate based curvature corrections tend to inhibit the convergence rate even more. The streamline-based correction seems to not have such an unfavourable effect in this case.

CONCLUDING REMARKS

Streamline curvature effects on turbulence exist in two-dimensional flows mainly in curved or rotating boundary layers. The ratio of the boundary layer thickness to the radius of curvature is a rough measure of the rate of influence on the turbulence. In high Reynolds number external flows, the curvature effect is not very large. However, the effect is rather easily captured by the curvature corrections proposed in this study, as well as corrections proposed in previous publications.

In three-dimensional flows, the flow topology often includes swirl and vortices, which may be strongly influenced by curvature and rotational effects. This is a much more difficult situation, but based on the computational results on the swirling combustor flow reported here, the effects can be captured by the curvature correction based on the strain-rate tensor proposed by Wallin & Johansson (2002). It is important that both the curvature correction itself and the EARSM are extended for three-dimensional flows.

In general the curvature correction proposed in this study has been shown to significantly improve the results compared to the standard EARSM. In many cases, the results are now much closer to the full RSM. However, the correction is rather complicated both due to complex algebraic expressions and due to the need of obtaining another level of derivatives of the velocity vector. The numerical stability is also somewhat degenerated.

The major argument of standard EARSM compared to full RSM is that the computational effort for computing complex three-dimensional cases using full RSM is very much reduced by using EARSM, which behaves numerically similar to standard eddy-viscosity models. By adding the curvature correction to the EARSM, this argument is not as clear anymore and one needs to be very careful in arguing for further extensions of the EARSM level of modelling.

Acknowledgment

This work has partly been carried out within the HiAer Project (High Level Modelling of High Lift Aerodynamics). The HiAer project is a collaboration between DLR, ONERA, KTH, HUT, TUB, Alenia, EADS Airbus, QinetiQ and FOI. The project is managed by FOI and is partly funded by the European Union (Project Ref: G4RD-CT-2001-00448).

References

Alvelius, K. & Johansson, A.V., 2000, Direct numerical simulation of rotating channel flow at various Reynolds numbers and rotation numbers. Submitted to *J. Fluid Mech.*, also in Doctoral thesis, Dept. of Mechanics, KTH, Stockholm, Sweden, 1999.

Bech, G.H. & Andersson, H.I., 1997 Turbulent plane Couette flow subject to strong system rotation. *J. Fluid Mech.*, **347**, 289–314.

Gatski, T.B. & Jongen, T., 2000, Nonlinear eddy viscosity and algebraic stress models for solving complex turbulent flows. *Progress in aerospace sciences*, **36**, (8), 655-682.

Gatski, T.B & Speziale C.G., 1993 On explicit algebraic stress models for complex turbulent flows. *J. Fluid Mech.* **254**, 59–78.

Girimaji, S.S., 1996 Fully-explicit and self-consistent algebraic Reynolds stress model *Theor. and Comp. Fluid Dyn.* **8** 387–402.

Girimaji, S.S., 1997 A Galilean invariant explicit algebraic Reynolds stress model for turbulent curved flows *Phys. Fluids.* **9** 1067–1077 (also *ICASE Report No. 96-38*).

Hellsten, A., 2002 Curvature corrections for algebraic Reynolds stress modeling: a discussion *AIAA Journal* **40** 1909–1911.

Hellsten, A., Wallin, S., & Laine, S., 2002 Scrutinizing curvature corrections for algebraic Reynolds stress models, in *32nd AIAA Fluid Dynamics Conference*, AIAA Paper 2002-2963.

Johansson, A.V. & Wallin, S., 1996 A new explicit algebraic Reynolds stress model. Proc. Sixth European Turbulence Conference, Lausanne, July 1996, Ed. P. Monkewitz, 31–34.

Monson, D.J., Seegmiller, H.L., McConnaughey, P.K., and Chen, Y.S., 1990 Comparison of experiment with calculations using curvature-corrected zero and two-equation turbulence models for a two-dimensional U-duct, in *AIAA 21st Fluid Dynamics, Plasma Dynamics and Lasers Conference*, AIAA Paper 90-1484.

Monson, D.J. & Seegmiller, H.L., 1992 An experimental investigation of subsonic flow in a two-dimensional U-duct. NASA TM 103931.

Roback, R. & Johnson, B.V., 1983 Mass and momentum turbulent transport experiments with confined swirling coaxial jets. NASA CR-168252.

Pope, S.B., 1975 A more general effective-viscosity hypothesis *J. Fluid Mech.* **72**, 331–340.

Rumsey, C.L., Gatski, T.L. & Morrison, J.H., 1999 Turbulence model predictions of extra-strain rate effects in strongly-curved flows. AIAA Paper 99-157

Rung, T., Lübcke, H., Xue, L., Thiele, F. and Fu, S., 1999 Assessment of explicit algebraic Reynolds-stress models in transonic flows, in *Engineering Turbulence Modelling and Experiments 4, Rodi, W. and Laurence, D. (editors).* Elsevier.

Salo, K., 2003 Implementing a Reynolds stress turbulence model in the FINFLO flow solver. Helsinki University of Technology, Laboratory of Aerodynamics, Report B-55.

Sjögren, T., 1997 Development and Validation of Turbulence Models Through Experiment and Computation Doctoral thesis, Dept. of Mechanics, KTH, Stockholm, Sweden.

Spalart P.R. & Shur, M., 1997 On the sensitization of turbulence models to rotation and curvature. *Aerospace Sci. & Tech.* **1**, (5), 297–302.

Speziale, C.G. & Mac Giolla Mhuiris, N., 1989 On the prediction of equilibrium states in homogeneous turbulence. *J. Fluid Mech.* **209**, 591–615.

So, R.M.C. & Mellor, G.L., 1973 Experiment on convex curvature effects in turbulent boundary layers. *J. Fluid Mech.*, **60**, 43–62.

Taulbee, D.B., 1992 An improved algebraic Reynolds stress model and corresponding nonlinear stress model. *Phys. Fluids A* **4**, 2555–2561.

Wallin, S. & Girimaji, S.S., 2000 Evolution of an isolated turbulent trailing vortex. *AIAA J.* **38**, 657–665.

Wallin, S., and Johansson, A., 2000, An explicit algebraic Reynolds stress model for incompressible and compressible flows. *J. Fluid Mech.* **403**, pp. 89–132.